Computational and Experimental Investigation of Flow in a Bileaflet Heart Valve with Leaflets in the Open Position

L. GE [1], H. L. LEO[2], J. CARBERRIE,[2] F. SOTIROPOULOS[1], & A. YOGANATHAN[2]
[1]School of Civil and Environmental Engineering, Georgia Tech, Atlanta, GA 30332-0355, USA
[2]Wallace Coulter School of Biomedical Engineering Engineering Georgia Tech, Atlanta, GA, *USA*

Abstract: - Direct numerical simulations are carried out for flow through a mechanical bileaflet heart valve with the leaflets fixed at the open position using a second-order accurate, domain decomposition method with overset (Chimera) grids. Results are reported for three Reynolds numbers, Re=350, 750, and 1200, and the computed solutions are analyzed to elucidate the increasing spatial and temporal complexity of the hemodynamics with Reynolds number. Digital particle image velocimetry experiments are also conducted and the measurements are employed to validate the numerical model. It is shown that the computations reproduce essentially all features of the measured velocity profiles with good accuracy.

Key-Words: - Bileaflet mechanical heart valves, cardiovascular flow, artificial organs, particle image velocimetry, computational fluid dynamics.

1 Introduction

Approximately 170,000 individuals worldwide receive prosthetic heart valves every year and over half (55%-65%) receive mechanical heart valves (MHVs). Recipients of MHVs, however, must take anticoagulant medication because of the potential for thromboembolic complications. Such complications are believed to be caused by high blood shear stresses, turbulence, and the overall complexity of hemodynamics in MHV. Computational fluid dynamics (CFD) modeling of MHVs promises to provide designers with a tool to refine existing MHV designs; however, the information provided by CFD must be accurate and reliable.

For the most part CFD modeling of the hemodynamics in MHVs has been limited to 2D studies [1-3] or 3D studies [1,3] with limited spatial resolution combined with the assumption of flow symmetry with respect to geometrical planes of symmetry. In a recent numerical study, Ge et al. [4] carried out calculations for a typical MHV geometry without adopting simplifying symmetry assumptions on grids that are at least one order of magnitude finer than those used in previously reported studies in the literature [4]. These computations illustrated the highly 3D structure of the flow, questioned the validity of computationally expedient assumptions of flow symmetry, and demonstrated the need for highly resolved, fully 3D simulations if CFD is to accurately predict the flow in MHV [4]. This work is motivated by the numerical findings of [4] and seeks to: 1) report the first validation of the numerical model by comparing model predictions with laboratory measurements; and 2) elucidate the complex physics of MHV flowfields with increasing Reynolds number.

Particle Image Velocimetry (PIV) experiments are conducted for various Reynolds numbers for a valve/aorta configuration identical to that used in the CFD model with the valve leaflets fixed at the open position. Fine-mesh, direct numerical simulations are carried out using a second-order accurate, overset grid numerical method [4]. The calculated velocity profiles are shown to be in excellent agreement with the measurements. The computed solutions are analyzed to investigate the mechanisms that lead to the onset of unsteadiness and three-dimensionality in the flow. It is found that the flow is dominated by pairs of streamwise vortices. The strength and number of these vortices grow with Reynolds number and above a threshold Re the complex interaction of these vortices leads to the break of quadrant symmetry and the onset of a dynamically rich unsteady flow. It is also found that the lateral straining imposed by these vortices on the major orifice jet causes it to switch its major and minor axes.

The paper is organized as follows. In section 2 we describe the numerical model and various

computational details. In section 3 we outline the experimental procedures. In section 4 we present the major features of the simulated flowfields and report the comparisons with the experimental measurements. Conclusions and areas of future research are presented in section 5.

2 The Numerical Method

We use a geometric model of a bileaflet MHV as a prosthetic for the aortic heart valve as shown in Figure 1. The primary simplification made in our geometric model is that the aortic root contains a single axisymmetric sinus and not three aortic sinuses. The leaflets in our model MHV closely resemble the St. Jude Medical (SJM) Standard valve. In the fully open position, the leaflets in the SJM standard valve make an angle of 85 degrees with x-y plane as shown in Figure 1(b,c).

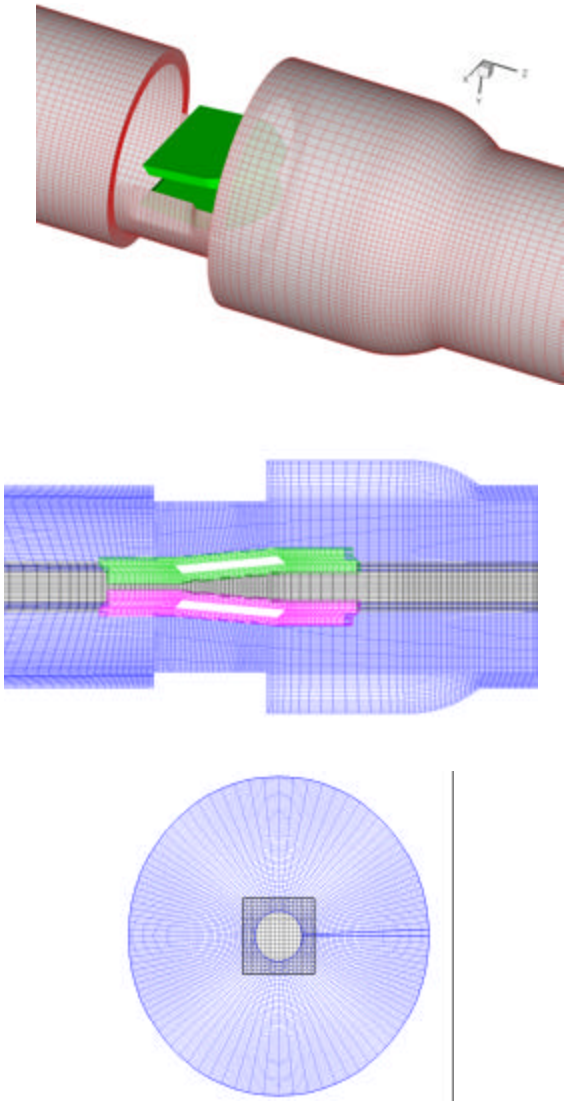

Figure 1. Aorta and leaflet geometry (top), overset grid layout in the streamwise (middle) and transverse (bottom) cross-sections.

To simulate this complex geometrical configuration, we use domain-decomposition method with structured overset (chimera) grids. Our method does not require one-to-one matching of grid lines across sub-domain interfaces, thus, permitting a great deal of flexibility. The details of the overset grid solver can be found in [4] and [5]. A cross-sectional view of the computational grid is shown Figure 1(c). The aorta geometry is discretized with a C-type circular grid plus an implemented squared block to resolve the singular point problem in the center. The dimensions of these two blocks are 67×102×135 and 21×21×135 in the x, y, and z directions respectively. The grid for each of the leaflets is a body-fitted H-H grid containing 81×21×65 nodes (approximately a total of 1.1×10^6 active nodes).

In each subdomain, the 3D incompressible Navier–Stokes equations are formulated in curvilinear coordinates and discretized in space using a three-point, second-order-accurate finite-volume scheme. Third-order, fourth-difference, artificial-dissipation terms are explicitly added to the discrete equations to suppress grid-scale oscillations. The discrete equations are integrated in time using a second-order-accurate, dual-time-stepping, pseudo-compressibility scheme. The Beam and Warming approximate-factorization scheme enhanced with local (dual) time stepping is employed to integrate the governing equations in pseudo-time. Typically 15 pseudo-iterations were required to reduce all residuals by three orders of magnitude. The unsteady simulations used a non-dimensional time step of 0.01. Non-reflecting, characteristic-based boundary conditions were applied at the outlet boundary to allow vortical structures to exit the flow domain without distortion. At the inlet boundary, a steady, fully developed velocity profile was specified. No-slip and no-flux conditions were specified on the rigid aorta walls and the leaflet surfaces.

3 Description of the Experiments

Flow experiments were performed on a St Jude Medical bi-leaflet mechanical heart valve. The valve

had a tissue annulus diameter of 23 mm, an orifice internal diameter of 20.4 mm and was geometrically identical to the prostheses implanted into patients. To facilitate visualization and measurement of the flow the valve was placed in a clear polycarbonate test section. Upstream of the valve the flow passed through a straight circular pipe, 1800 mm in length, ensuring that the flow entering the test section had a fully developed profile, thus the entrance profile matched that used in the numerical calculations. The fluid used in the experiment (79% saturated aqueous sodium iodide, 20% glycerin and 1% water by volume) is a blood analog having the same kinematic viscosity as blood at high shear, 3.5 cSt,

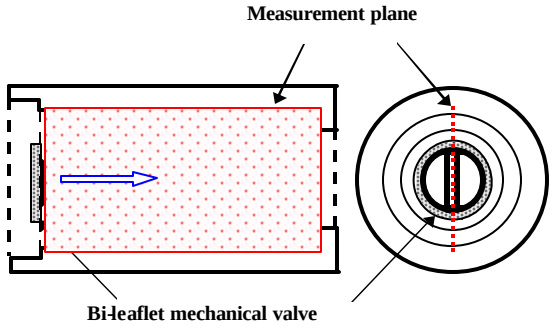

Figure 2: Sketch of experimental geometry showing the location of the central measurement plane

but is transparent allowing the measurement of flow velocities using the PIV technique. The refractive index of the fluid was matched to that of the experimental chamber to reduce optical distortion. The flow was seeded with 10 μm silver coated glass spheres and the data plane was illuminated using a 532 nm Nd:YAG laser.

Steady flow measurements were taken at five different upstream flow velocities corresponding to Reynolds numbers of Re = 350, 750, 1250, 3000, and 5800. Thus the experimental parameters cover the full range of Reynolds numbers observed during forward flow through a valve during pulsatile flow in a resting healthy adult. Two-dimensional PIV was performed using a TSI Insight © system resulting in the measurement of velocity vectors in a plane centered on the valve, as shown in Figure 2, along a 75 mm long section of the chamber. A sequence of 300 flow fields was acquired in order to characterize both the mean and fluctuating velocity components. In order to fully characterize the flow set of measurements was obtained for each of the 5 Reynolds numbers.

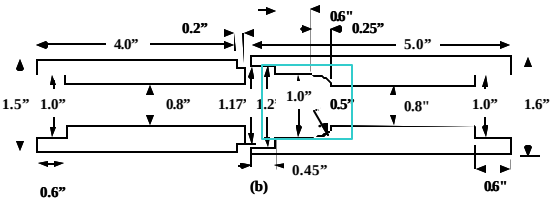

Figure 3: Sketch with dimensions and measurement window marked.

4 Results and Discussion

We have carried out time-accurate numerical simulations for various Reynolds numbers between 300 and 1250—the Reynolds number is based on the bulk velocity at the inlet and the diameter of the model aorta. For Reynolds numbers less than approximately 325 the simulations approached steady-state and converged steady solutions were obtained. These solutions exhibited symmetry with respect to the axes of symmetry of the valve and will not be discussed here. For Reynolds number greater than 325, however, weak unsteady modes began to emerge naturally without any externally imposed forcing other than numerical disturbances in the numerical approach. The unsteadiness at this low Reynolds number was weak but it was sustained over a long simulation interval. The strength of the unsteady fluctuations and the richness of the flow were found to increase continuously with Reynolds number. It is important to note that in this study unsteady flow sets in at Reynolds numbers considerably lower than those reported in [4]. This trend should be attributed to the different aortic root geometry we employed in this work and underscores the sensitivity of the MHV flowfields to the details of the aortic root geometry.

To quantify the onset of unsteadiness in the flow, we show in Figs. 4 and 5 time series and the corresponding power spectrum of the vertical velocity component at the center of a cross-section downstream of the leaflets for Re = 350 and 750, respectively. Note that regardless of whether the flow is steady or unsteady, if it preserves the quadrant symmetry of the valve geometry the two transverse velocity components at the center of any cross-section should remain equal to zero at all times. As seen in Fig. 4a, weak unsteady fluctuations emerge for Re=350 which also signify the break of quadrant symmetry. A rather interesting feature that follows from Fig. 4a and the corresponding power spectrum shown in Fig. 4b is the fact that the flow does not undergo a simple,

periodic temporal oscillation. Rather the unsteadiness appears to be quasi-periodic in nature with two incommensurate frequencies. A similar trend is also observed for Re=750 (see Fig. 5). At this higher Reynolds number, however, both the complexity and amplitude of the fluctuations about the zero mean increase considerably as compared to those for Re=350.

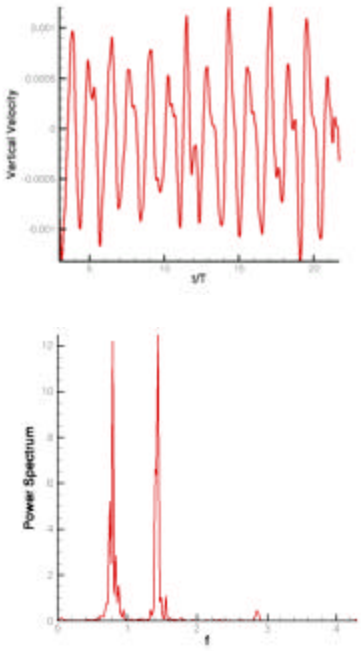

Figure 4. Time series and spectra of the vertical velocity component at the center point downstream of the leaflets for Re=350

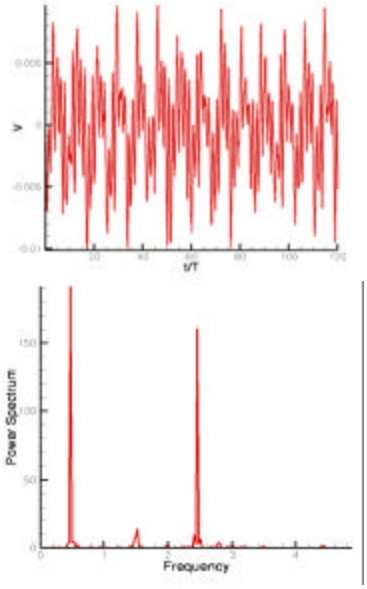

Figure 5. Time series and spectra of the vertical velocity component at the center point downstream of the leaflets for Re=350

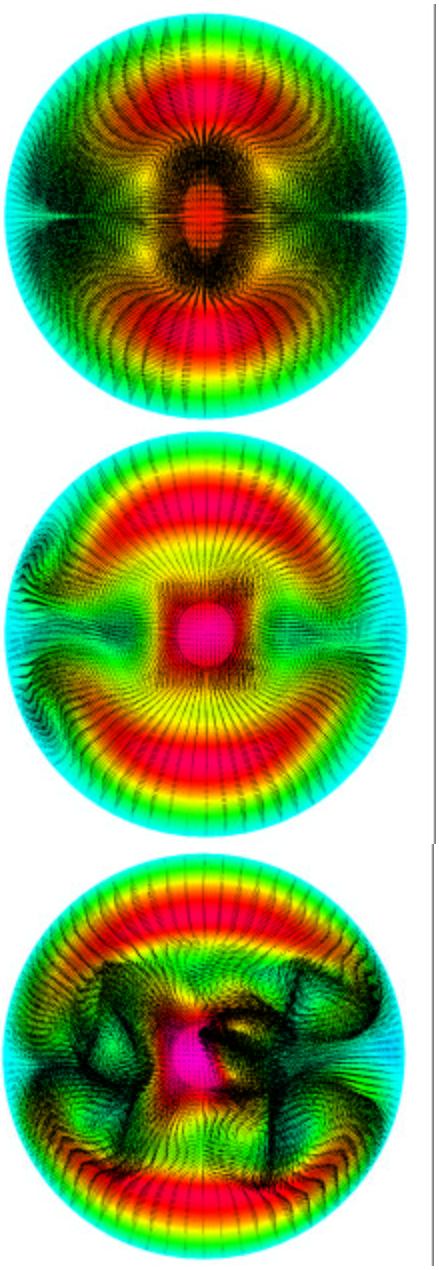

Figure 6. Instantaneous snapshots of streamwise velocity contours and cross-flow vectors at a cross-section downstream of the leaflets for Re=350 (top), 750 (middle), 1200 (bottom).

To elucidate the mechanism that leads to the onset of unsteadiness in the flow, we plot in Fig. 6 instantaneous snapshots of cross-flow vectors and streamwise velocity contours at a cross-section downstream of the leaflets for Re = 350, 750, and 1250. For Re =350 two pairs of streamwise vortices emerge downstream of the leaflets near the right and left sides of the aorta. These vortices transport low momentum fluid from the aortic wall toward the center of the cross section leading to the

characteristic bulging of the isovels in this region. The vortices also act to strain laterally the major orifice jet causing to switch its major axis from the horizontal to the vertical direction. This important phenomenon will be discussed in more detail subsequently in this section. For Re=350 the two vortical pairs begin to oscillate in time around their fixed mean positions but without altering the basic structure of the flow. For Re=750, however, the vortices begin to undergo much stronger fluctuations and there are instants in time when two new counter-rotating vortical pairs are extracted because of the interaction between the main vortices and the aortic wall (see Fig. 6b). For the highest Reynolds number simulate din this work (Re=1200), the cross-flow pattern becomes very disorganized with multiple pairs of vortices appearing and disappearing seemingly randomly in time. These vortices cause rather severe deformation of the major jet as suggested by the snapshot shown in Fig. 6c.

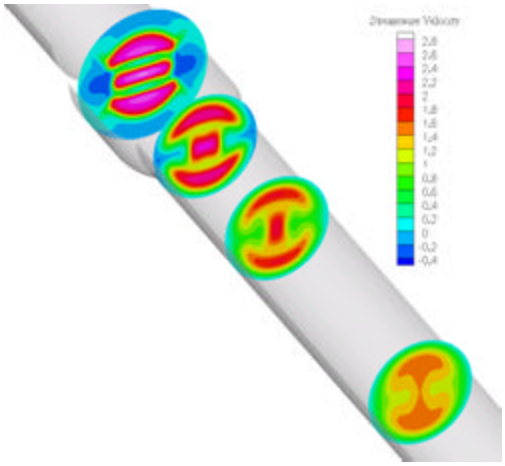

Figure 7. Instantaneous streamwise velocity contours at various cross-sections showing the switching of the major orifice jet axes (Re = 750).

As discussed above, the vortices that emerge downstream of the leaflets interact with the major orifice jet and cause it to switch its major axis. This complex phenomenon is well documented in the literature for rectangular jets in free-shear flows but has never been discussed before in the context of MHV flows. Fig. 7 shows instantaneous snapshots of streamwise isovels at several cross-sections downstream of the leaflets for Re=750. These snapshots clearly show the spatial evolution of the main orifice jet from a laterally stretched, rectangular-like jet to a vertically oriented jet. The figure also shows the ultimate merging of major orifice jet with the two minor orifice jets downstream of the leaflets. To the best of our knowledge this is the first time that this complex phenomenon has been documented either computationally or experimentally in MHV flows.

To demonstrate the predictive capabilities of the model we compare in Fig. 8 time-averaged, streamwise mean velocity profiles for the Re=750 case (for measurement locations see Fig. 3). As seen in the figure, the simulated velocity profiles capture with remarkable accuracy all aspects of the measured flow, including both the transverse distribution of momentum within the cross-section and the rate at which the three jets diffuse in the streamwise direction.

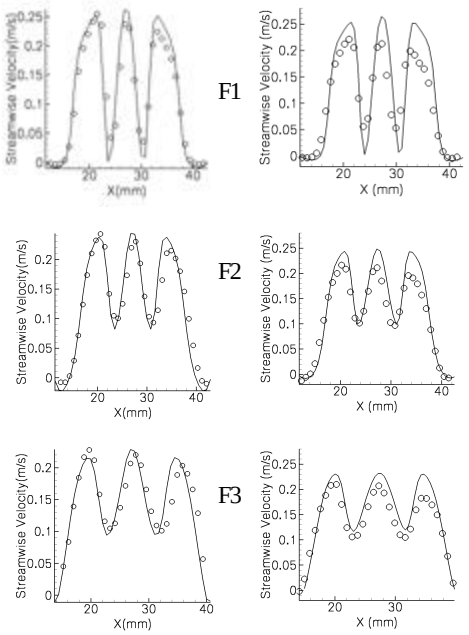

(a) Center plane (b) 0.15d from the center

Figure 8. Comparisons of measured and calculated time-averaged streamwise velocity profiles.

6 Summary and Conclusions

We have reported a combined experimental and computational study of flow in a MHV with the leaflets fixed in the fully open position. Our results reinforce are earlier finding [4] regarding the complexity of MHV flows even at relatively low Reynolds numbers and underscore the need for an integrated research strategy combining high resolution CFD modeling with laboratory experiments.

To the best of our knowledge this is the first time that the predictive capabilities of a numerical for

MHV flows have been demonstrated to the level of detail, which has been accomplished in this work. Yet, the complexity of the flow downstream of the leaflets suggests that the validation presented in this work, encouraging as it may be, can only be considered as preliminary. Highly resolved unsteady measurements over a broad range of Reynolds numbers will be needed to validate the wealth of information obtained by the numerical model and demonstrate that our numerical approach can evolve into a powerful simulation tool for understanding the hemodynamics of heart valves and improving their designs.

Our future work will focus on systematic investigation of the flow at progressively higher Reynolds numbers both experimentally and computationally. After we have demonstrated the ability of the model to accurately predict the flow for the fixed-leaflet case, we will undertake a systematic investigation of the pulstatile flow at physiological Reynolds numbers.

Acknowledgement

This work was supported by NIH grant R01-HL-07262.

References:

[1] Aluri S, Chandran KB. Numerical simulation of mechanical mitral heart valve closure. *Annals of Biomedical Eng.* 2001; 29:665-676.

[2] Lai YG, Chandran KB, Lemmon J. A numerical simulation of mechanical heart valve closure fluid dynamics. *J. of Biomechanics* 2002; 35:881-892.

[3] Rosenfeld M, Avrahami I, Einav S. Unsteady effects on the flow across tilting disk valves. *ASME J. Biomechanical Eng*., 2002; 124:21-29.

[4] Ge, L., Jones, S. C., Sotiropoulos, F., Healy, T., and Yoganathan, A. Numerical Simulation of Flow in Mechanical Heart Valves: Grid Resolution and Flow Symmetry. *ASME J. of Biomechanical Eng.*, 125(5): 709-718, 2003.

[5] Tang, H., Jones, S. C., and Sotiropoulos, F., "An Overset Grid Method for 3D, Unsteady, Incompressible Flows," *J. Comp. Physics*, 191(2), 567-600 2003.